

Electronic Supporting Information (ESI)

Experimental Section

A) Materials

Commercial hydrophobic CdSe/CdS quantum rods (QRs, CANdots, consisting a dot in a rod core/shell structure type, two batches with a λ_{EM} of ~ 550 and ~ 570 nm, respectively, quantum yield = 68%, supplied as 20 μM stock in hexane) were purchased from Strem Chemicals UK Ltd (Cambridge, UK). CdSe/ZnS core/shell QD ($\lambda_{EM} = \sim 600$ nm) was purchased from PlasmaChem GmbH (Berlin, Germany). The QD was supplied as dry powders capped with mixed ligands of trioctylphosphine oxide (TOPO), hexadecylamine and oleic acid. Hoechst 33342 was purchased from Thermo Fisher. Polyethylene glycol (PEG) with an average molecular weight of 600 (containing an average of ~ 13 PEG units, denoted as PEG₁₃); N,N-dimethyl-1,3-propanediamine (>99%), 1,3-propanesultone (>99%), triphenylphosphine (>98.5%), dicyclohexylcarbodiimide (DCC, >99%), dimethylaminopyridine (DMAP >99%), lipoic acid (LA >99%), tris(2-carboxyethyl)phosphine hydrochloride (TCEP.HCl, >98%), triethylamine (>99%), chloroform (> 99.8%), magnesium sulfate (>99%), methanol (>99.9%), potassium hydroxide, ethylacetate (>99.0%), methylene chloride (>98%), sodium bicarbonate (>99.5%), Roswell Park Memorial Institute (RPMI 1640) medium, fetal bovine serum (FBS), penicillin, tpsin-EDTA, Dulbecco's phosphate buffered saline (PBS) and other chemicals were all purchased from Sigma-Aldrich (Dorset, UK) and used as received unless stated otherwise. Solvents were obtained from Fisher Scientific (Loughborough, UK) and used as received unless stated otherwise. Ultra-pure water (resistance >18.2 M Ω .cm) purified by an ELGA Purelab classic UVF system, was used for all experiments and making buffers.

B) Instrument and Methods^{1,2}

All moisture sensitive reactions were performed under nitrogen atmosphere using oven dried glassware. Dry solvents were obtained through an innovative technology solvent drying system. Evaporations were performed under reduced pressure on a rotary evaporator. The synthesis was monitored by TLC on silica gel 60 F254 plates on aluminum and stained by iodine. Column chromatography was performed on silica gel 60 A (Merck grade 9385) on gravity flow. All ¹H and ¹³C NMR spectra were recorded on Bruker DPX300 (500 MHz for ¹H, 125 MHz for ¹³C) in CDCl₃. All chemical shifts were reported in

parts per million (ppm) and the coupling constants were given in Hz. High resolution mass spectra (HR-MS) were obtained on a Bruker Daltonics MicroTOF mass spectrometer. UV-vis absorption spectra were recorded on a Varian Cary 50 bio UV-Visible Spectrophotometer over a range of 200-800 nm using 1 mL quartz cuvette with an optical path of 1 cm or on a Nanodrop 2000 spectrophotometer (Thermo Scientific) over the range of 200-800 nm using 1 drop solution with an optical path length of 1 mm. All centrifugations were carried out on a Thermo Scientific Heraeus Fresco 21 microcentrifuge using 1.5 mL microcentrifuge tubes at room temperature. Dynamic light scattering (DLS) was measured using Zetasizer Nano (Malvern) using the volume size distribution function as described previously.^{1,2} All fluorescence spectra used for target protein detection were measured on a Spex Fluoro Max-3 Spectrofluorometer using a 0.70 mL quartz cuvette under a fixed excitation wavelength (λ_{EX}) of 450 nm. This wavelength corresponds to the absorption minimum of the acceptor dye, Atto-594, to minimize the direct excitation background of the acceptor.¹ The direct excitation background, despite small, was corrected from the resulting fluorescence spectra using the same concentration dye labelled protein only under identical experimental conditions. An excitation and emission band widths of 5 nm and a scan rate of 120 nm/min over 480-800 nm range were used.

C) Ligand synthesis³⁻⁵

Lipoic acid zwitterion (LA-ZW) ligand was synthesised and purified by HPLC and lyophilized to give a yellow powder in 23% yield as described previously.^{3,4} ¹H NMR (300 MHz, D₂O): δ (ppm) 3.60-3.70 (m, 1H), 3.40-3.50 (m, 2H), 3.28-3.35 (m, 2H), 3.20-3.28 (m, 2H), 3.10-3.20 (m, 2H), 3.10 (s, 6H), 2.90 (t, 2H), 2.40-2.50 (m, 1H), 2.20 (t, 2H), 2.15 (m, 2H), 1.93-2.0 (m, 2H), 1.70 (m, 1H), 1.50-1.60 (m, 4H), 1.35-1.40 (m, 2H).

LA-PEG₆₀₀-biotin was synthesised as a waxy solid in 51% yield as described in our recent paper.⁵ ¹H NMR (300 MHz, CDCl₃): δ (ppm) 6.79-6.98 (m, 1H), 6.43-6.65 (m, 1H), 5.65-5.85 (m, 1H), 4.92-5.12 (m, 1H), 4.47-4.63 (m, 1H), 4.33 (m, 1H), 3.5-3.9 (m), 3.40-3.50 (m, 2H), 3.10-3.20 (m, 3H), 2.80-2.98 (m, 1H), 2.75 (d, 1H), 2.40-2.60 (m, 1H), 2.10-2.30 (m, 4H), 1.80-1.96 (m, 1H), 1.60-1.80 (m, 8H), 1.40-1.60 (m, 4H). LC-MS gave a series of peaks separated by 44 m/z units, corresponding to different PEG chain lengths in the mixed length PEG₆₀₀ linker, e.g. 1048.0, 1004.8, 959.6, 915.7, 871.7. The calculated corresponding [M+H]⁺ peaks for LA-PEG_n-Biotin where n = 13, 12, 11, 10 and 9 were 1048, 1004, 959, 915 and 871, respectively. The double charge peaks were stronger at m/z values of 568.4,

546.4, 524.4, 502.4, 480.4, 458.4, 436.4 and 414.4, corresponding to the $[M + 2H]^{2+}$ with $n = 15, 14, 13, 12, 11, 10, 9, 8,$ and $7,$ respectively.

D) Preparation, characterisation and cellular imaging of QR

D1) Preparation of DHLA-Zwitterion ligand capped QR (QR-ZW)

Commercial CdSe/CdS QR (0.2 nmole, 10 μ L in hexane, $C = 20 \mu$ M as provided by the supplier) was precipitated by adding 500 μ L EtOH, followed by centrifugation to remove any unbound free ligands. The QR pellet was then dissolved in 100 μ L $CHCl_3$ and then added with 50 μ L EtOH to make solution **A**. The LA-ZW ligand (0.10 M, 2 μ L in H_2O) was reduced to DHLA-ZW by mixing with TCEP.HCl (0.10 M, 2 μ L in H_2O) for 15 mins. After which NaOH (0.10 M in EtOH, 12 μ L) was added to deprotonate the DHLA thiol groups and to neutralise acid groups in TCEP.HCl (each containing 4 acid groups) to make solution **B**. Solutions **A** and **B** were then mixed for ~ 1 min with shaking by hand. After that, the reaction mixture was centrifuged (1000 rpm for 10 s) and the QR was found to form a pellet at the bottom of the tube, leaving the supernatant colourless. After careful removal of the supernatant, the QR pellet was dissolved in H_2O (100 μ L) to yield a clear, homogeneous stock solution. The QR stock concentration was determined by Beer-Lambert Law from its UV-vis absorbance at its first exciton peak (~ 545 nm) using an extinction coefficient ($\epsilon = 2.56 \times 10^5 \text{ M}^{-1}\text{cm}^{-1}$).⁵ The ϵ value was determined from the original stock concentration provided by the supplier (20 μ M) and its UV-vis spectrum.

D2) Preparation of DHLA-PEG₆₀₀-biotin ligand capped QR (QR-biotin_x)

Hydrophobic QR (0.20 nmol, 10 μ L in hexane) was precipitated by adding 500 μ L EtOH and centrifuged to remove any unbound free ligands. The QR pellet was then dissolved in a 100 μ L $CHCl_3$ and then added with 60 μ L EtOH to make solution **A**. LA-ZW (0.10 M, 2 μ L in H_2O) and LA-PEG₆₀₀-biotin (0.01 M, 4 μ L in EtOH) were mixed with TCEP (0.10 M, 2.4 μ L in H_2O) for ~ 20 mins to reduce to their DHLA-equivalents, after that NaOH (0.10 M in EtOH, 14.4 μ L) was added to deprotonate the DHLA thiol groups and to neutralise acid groups in TCEP to make solution **B**. Solutions **A** and **B** were then mixed for ~ 1 min with occasional shaking by hand. After centrifugation, the QR pelleted to the bottom of the tube. After careful removal of the clear supernatant, the QR pellet was dissolved in pure H_2O (50 μ L) to give a clear stock solution. Its concentration was determined by the same method above.

D3) Affimer and SUMO protein production and labeling

The yeast SUMO (SUMO) protein and the anti-SUMO Affimers were expressed in BL21 (DE3) cells using isopropyl β -D-1-thiogalactopyranoside (IPTG) induction and purified by Ni-NTA resin (Qiagen) affinity chromatography according to the manufacturer's instructions as described previously.⁶

Protein labelling. The anti-SUMO Affimer (5 mg/mL, 12.5 μ L in PBS, MW = 13,267) in an Eppendorf tube was first mixed with Atto 594 NHS-ester (30 μ g in 2 μ L DMSO), then 5 μ L NaHCO₃ (0.5 M, pH = 8.3) and 7.5 μ L PBS (10 mM phosphate, 150 mM NaCl, pH 7.4) were added and thoroughly mixed (dye:protein molar ratio \approx 4:1). The resulting solution was allowed to stand at room temperature overnight. After that, the reaction mixture was loaded on a small G25 gel filtration column using PBS as the eluting solution on natural flow. The first eluted purple band (corresponding to the labeled anti-SUMO Affimer) was collected and its UV-vis spectrum was recorded. Using the extinction coefficients of the Atto-594 dye (120,000 M⁻¹cm⁻¹ at 601 nm) and Affimer (7904 M⁻¹cm⁻¹ at 280 nm) and the CF280 nm of 0.51 for Atto-594, the average dye labeling ratio per Affimer was calculated as 0.35. The stock protein concentration was determined as 8.4 μ M.

Similarity, the SUMO protein was labelled with Atto-594 NHS ester using the same procedures as above at a dye:protein molar ratio of 5:1. After purification on a G25 column as above, the average dye label per protein was determined as 0.25. The labeled protein stock concentration was 10 μ M.

D4) Neutravidin labelling⁷

Neutravidin (28.8 μ L, 10 mg/mL, MW = 60,000 Daltons) in an Eppendorf tube was added Atto-594 NHS ester (50 μ g in 2 μ L DMSO) and then 7.5 μ L PBS (10 mM phosphate, 150 mM NaCl, pH 7.4) was added and thoroughly mixed (protein:dye molar ratio \approx 1: 8). After standing at room temperature for 8 h, the mixture was purified on a small G25 gel filtration column using PBS as eluting solution on natural flow. The first eluted purple band (labelled Neutravidin) was collected and the dye label per protein was calculated as 0.67 using the above method. The stock protein concentration was 4.6 μ M.

D5) Cell culture, cell based studies and imaging⁵

Cell Culture: 4T1 breast cancer cells were grown in the Roswell Park Memorial Institute medium (RPMI 1640) supplemented with 10% (v/v) fetal bovine serum (FBS) and 100 U mL⁻¹ penicillin/streptomycin and maintained in a humidified incubator at 37°C with 5% CO₂.

Laser scanning confocal microscopy: 2 mL of 4T1 cells (1.5×10^5 cells mL⁻¹) were cultured for 24 h followed by the treatment with 1 mL of the serum free RPMI 1640 with or without of the QR sample

(50 nM). After 4 h incubation, cells were washed three times with Dulbecco's phosphate buffered saline. Hoechst 33342 was added to a final concentration of 5 $\mu\text{g mL}^{-1}$ for nuclei staining. The cells were then imaged by laser scanning confocal microscopy (Zeiss LSM-510 inverted laser scanning confocal microscope, Germany). The cellular QR fluorescence image was obtained using 488 nm laser excitation and collecting emission above 525 nm was collected using a long path filter.

D6) Femtosecond transient absorption measurements⁸

Briefly, we used an amplified Ti:sapphire laser system (Spitfire, Spectra Physics, Mountain View, CA), which generated about 100 fs laser pulses at 800 nm with a repetition rate of 1 kHz and an average power of ~ 1.0 W. These fundamental pulses were used to pump an optical parametric amplifier (OPA) as well as to generate a continuous white light. The OPA pulses were about 100 fs and could be tuned from 450 to 700 nm. The white light continuum was generated in a spinning fused-silica disk with the 800 nm pump pulse and its spectrum covered the range from 420 to 750 nm. The OPA outputs were used as the pump pulses, and the white light continuum were used as the probe pulses. The timing between the pump and probe pulses was controlled using a motorized translation stage (M-ILS250CC, Newport, Irvine, CA). The pump and probe beams were non-collinearly focused into the sample cell using two achromatic lenses (300 mm focal length for pump and 100 mm focal length for probe, respectively). At the sample position, the average powers were about 0.5 mW for pump beam, and around 10 μW for the white light continuum probe beam. The signals were collected by a large area adjustable gain balanced photo-receiver (2307, Newport, Irvine, CA) which was attached to the output port of a monochromator (SP2358, Princeton Instruments, Acton, MA) and sent to a lock-in amplifier (SR850, Stanford Research Systems, Sunnyvale, CA), where it was synchronized by an optical chopper (75160, Newport, Irvine, CA). The chopped frequency was 160 Hz. The polarization of the pump pulses was set at 54.7° with respect to the polarization of the probe pulses to remove the molecular re-orientation effect. The time resolution for this femtosecond transient absorption apparatus was estimated to be about 150 fs through the cross correlation between the pump and probe pulses in buffer solution. The transition absorption spectrum was recorded at a time delay of 2 ps by scanning the monochromator from 420 to 630 nm on the QR sample with a concentration of about 1 μM . To ensure that the sample solution was uniform during the measurement, a homemade magnet stirring bar was placed inside a 1 mm optical path length sample cell and rotated by an external magnet motor.

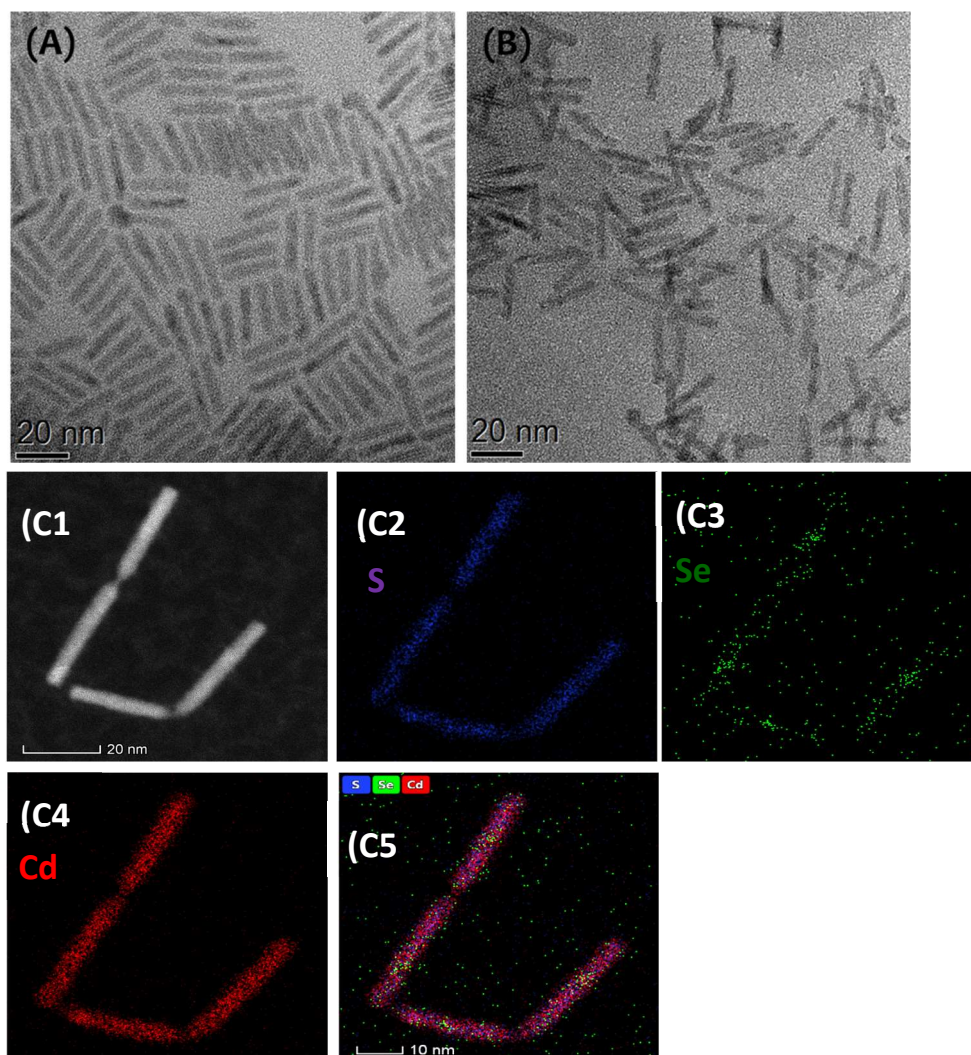


Figure S1. (A) TEM image of the commercial CdSe/CdS core/shell QR ($\lambda_{EM} \sim 550$ nm) before cap-exchange showing an approximately size of 3.6 nm wide (D) and 24 nm long (L). (B) A TEM image of the QR after cap-exchange with DHLA-ZW ligand at a ligand:QR molar ratio of 1000:1, no apparent change of the QR size is observed. (C) A S/TEM image (C1) and the corresponding EDX maps of the QR elements with S showing in blue (C2), Se in green (C3); Cd in red (C4), and overlay of the three elements (C5). The Se signal is weak but can be seen mostly centered in the centre of the QR, which is consistent with a CdSe dot in a CdS rod structure. Data was collected using a FEI Titan Themis G2 S/TEM operating at 300 kV fitted with 4 EDX detectors and a Gatan OneView. EDX mapping was undertaken using a probe current of 750 pA and Velox software.

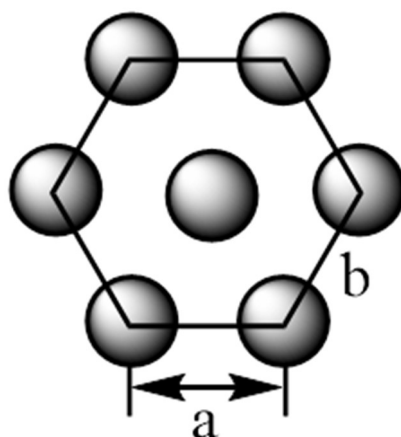


Figure S2. Estimation the number of surface Cd^{2+} ions and ligands required to cap each CdSe/CdS core/shell QR (width $D = 3.6$ nm, length $L = 24$ nm).

Assuming CdS in stable Wurtzite structure with a hexagonally packed Cd^{2+} outer layer, where $a = b = 0.416$ nm.¹⁰

The number of Cd^{2+} ions in the hexagon = $1 + 6 \times (1/3) = 3$.

Area of the hexagon = $6 \times (1/2) a^2 \times \sin 60^\circ = 3 \times 0.416^2 \sin 60^\circ = 0.450$ nm²

Footprint of each Cd^{2+} ion = $0.450/3 = 0.150$ nm²

Total surface area of each QR = $2 \pi (D/2)^2$ (bottom surfaces) + $\pi \times D$ (width) $\times L$ (length) (side surfaces)
 $= 2 \times 3.14 \times 1.8^2 + 3.14 \times 3.6 \times 24 = 291$ nm²

The number of surface Cd^{2+} ions on each QR = $(291/0.150) = 1940$.

Assuming each thiolate binds to one Cd^{2+} ion, then 1940 mono-thiolate ligands or 970 DHLA-based ligands (each containing 2 thiol groups) would completely saturate all the QR surface Cd^{2+} ions.

This number matches well to our observation that a LQMR of 1000 is sufficient to completely water-disperse the QR to give stable, homogeneous and aggregation-free QRs, suggesting that most of the added DHLA-ligands have bound to the QR surface.

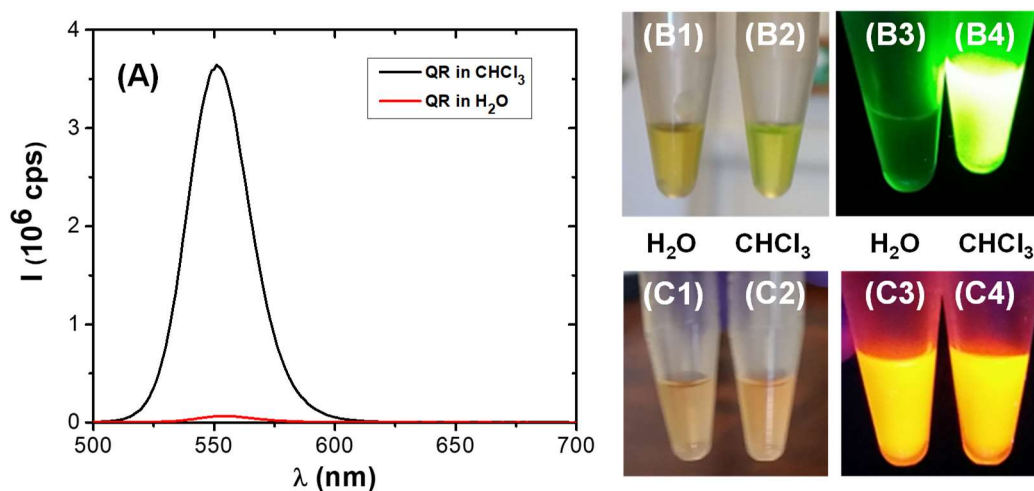


Figure S3. (A) Fluorescence spectra ($\lambda_{\text{EX}} = 450 \text{ nm}$) of 1 nM CdSe/CdS core/shell QR before (black, in CHCl_3) and after (red, in H_2O) cap-exchange with DHLA-ZW ligand at 1000 LQMR, revealing a dramatic decrease of fluorescence intensity by >98%. (B) Photographs of 1 nmole CdSe/CdS core/shell QR after (B1, B3, in H_2O) and before (B2, B4, in CHCl_3) cap-exchange with DHLA-ZW ligand at 1000 LQMR under ambient room light (B1, B2) and UV light (B3, B4) illumination. (C) Photographs of 1 nmole CdSe/ZnS core/shell QD after (C1, C3, in H_2O) and before (C2, C4, in CHCl_3) cap-exchange with the DHLA-ZW ligand under ambient room light (C1, C2) and UV light (C3, C4) illumination.

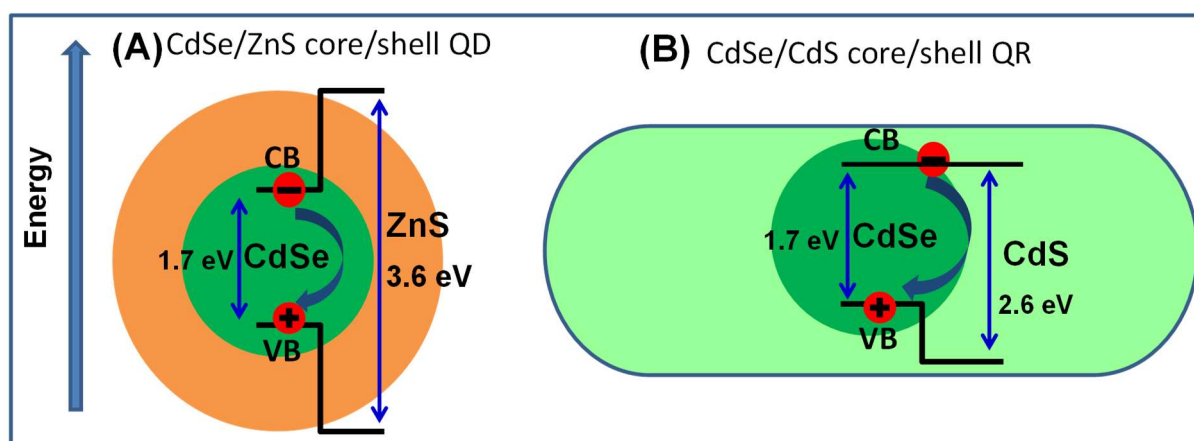


Figure S4. Schematic energy level alignments of the core and shell materials of different core/shell structures. (A) A CdSe/ZnS type I QD: both electron and hole are confined within the core, giving rise to core-core recombination. (B) A quasi-Type II CdSe/CdS QR: the hole is confined in the core, but the electron is spread across the whole core/shell structure, giving rise to a core/shell to core recombination.

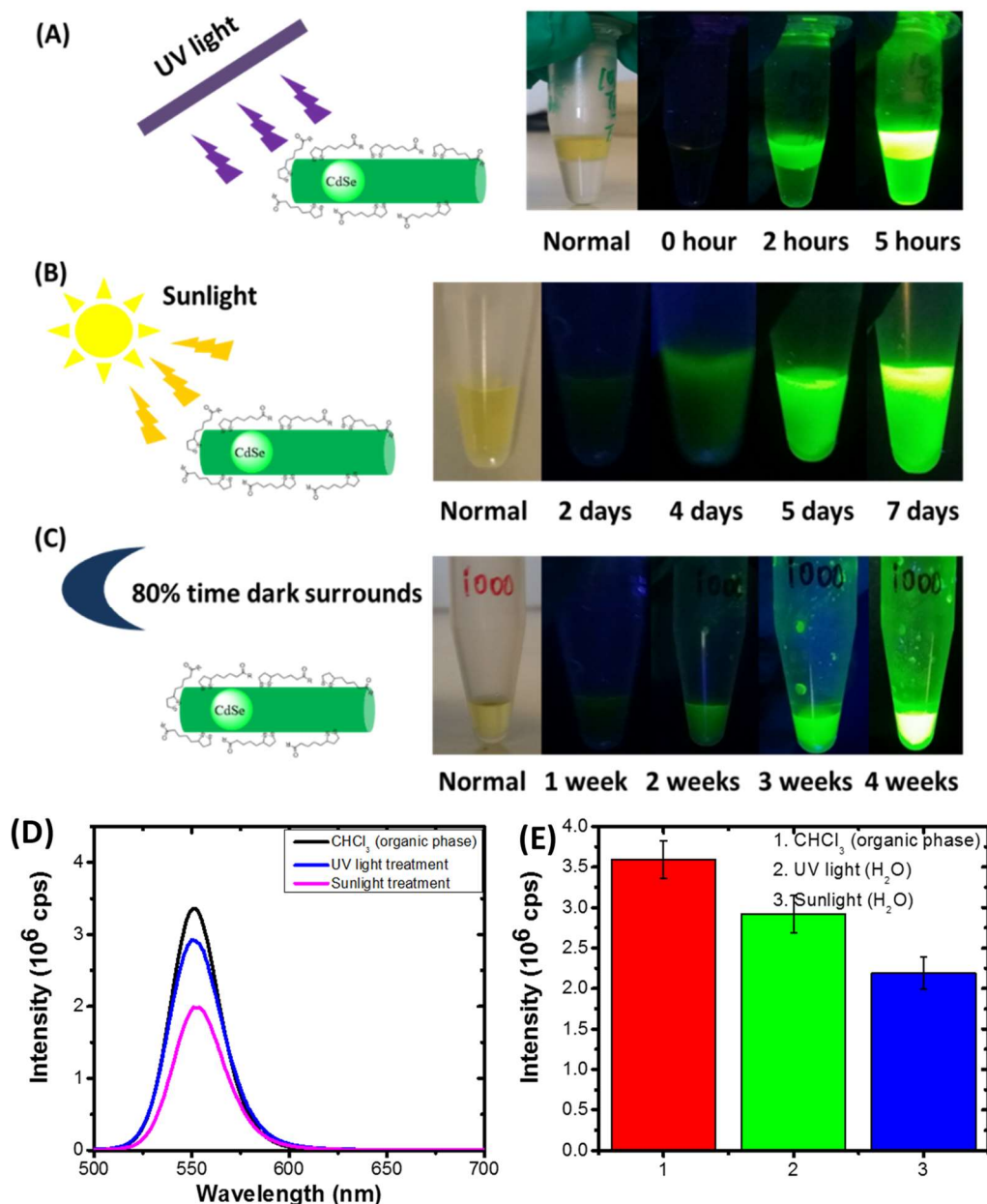


Figure S5. Photographs showing the time-dependent fluorescence recovery of a DHLA-ZW ligand capped CdSe/CdS QR ($\lambda_{EM} \sim 550$ nm) exposed to different light conditions: **(A)** a TLC UV lamp ($\lambda = 365$ nm, top layer: H_2O , bottom layer: $CHCl_3$); **(B)** ambient room light, and **(C)** in darkness wrapped with aluminium foil with occasional exposure to room light (due to inspection). All photographs were taken under UV illumination ($\lambda = 365$ nm), except those labelled as normal which were taken under ambient room light.

(D) Fluorescence spectra ($\lambda_{EX} = 450$ nm) of the parent QR (black, in $CHCl_3$) and cap-exchanged with DHLA-ZW at 1000 LQMR in H_2O after photon regeneration with UV light (blue) or ambient sun light (pink). **(E)** Comparison of their relative fluorescence intensities, error bars show the standard deviations of three samples.

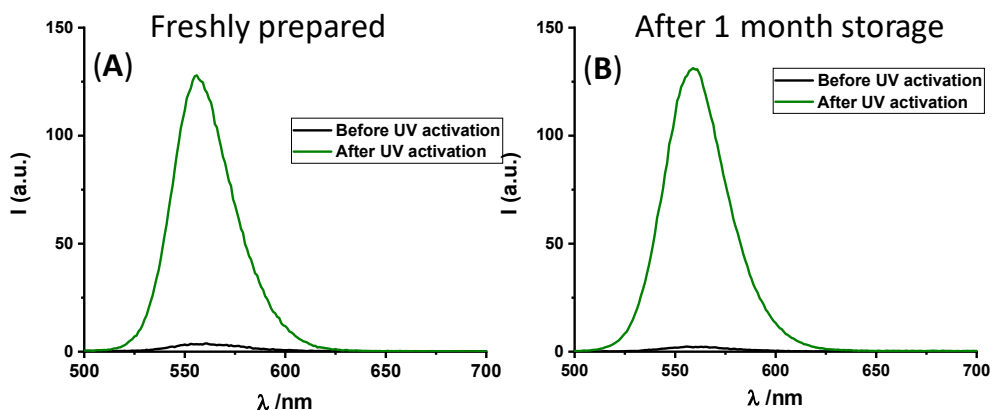


Figure S6. (A) Fluorescence spectra ($\lambda_{\text{EX}} = 450$ nm) of a freshly prepared DHLA-PEG₇₅₀ capped QR before (black) and after (green) 4 h UV activation with a TLC UV lamp ($\lambda = 365$ nm). (B) Fluorescence spectra of the same QR samples after 1 month storage in darkness (wrapped in aluminum foil) at room temperature. All $C_{\text{QR}} = 20$ nM.

Table S1. Summary of the photon activation rate at the rapid linear activation stage of a DHLA-ZW capped-CdSe/CdS QR under repeated emission scans of a given λ_{EX} .

λ_{EX} (nm)	Increase rate (10^3 cps/scan)	R^2
300	22.7 ± 0.5	0.995
350	48.5 ± 0.4	0.998
400	69.5 ± 0.9	0.996
450	29.5 ± 0.3	0.996
500	/	/

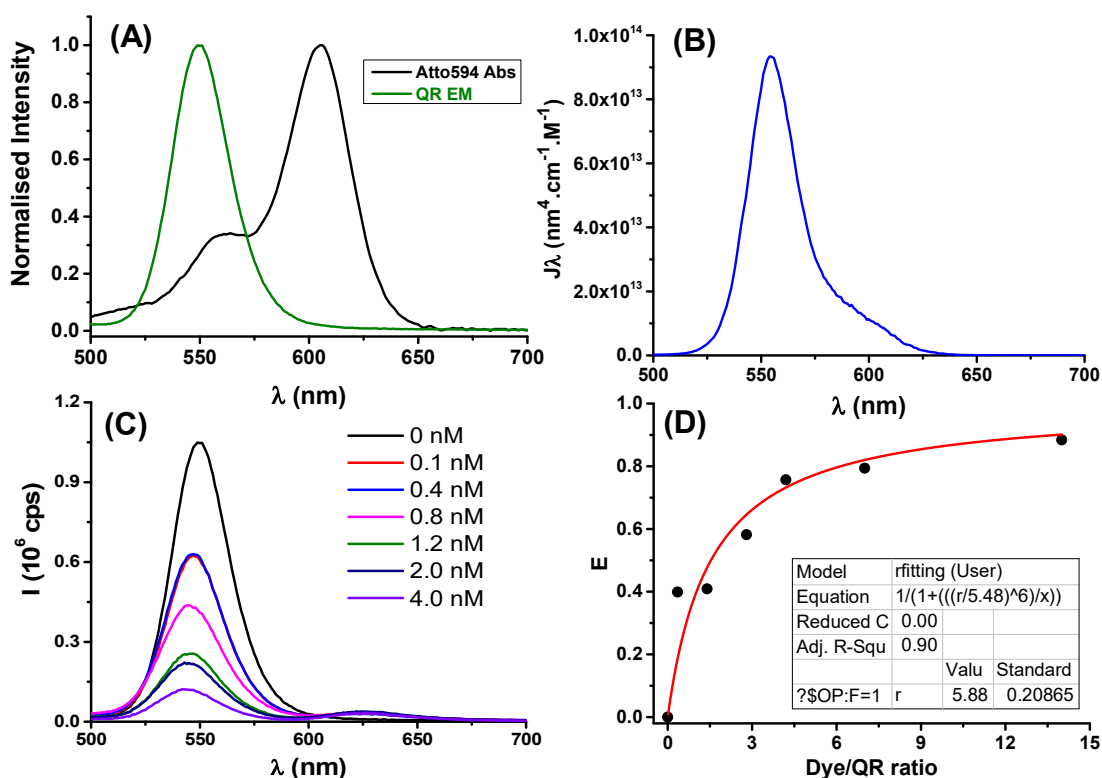


Figure S7. (A) Normalised CdSe/CdS QR fluorescence (green) and Atto-594 absorption (black) spectra, and (B) their spectral overlap function as a function of wavelength. (C) Fluorescence spectra ($\lambda_{\text{EX}} = 450$ nm) of QR-ZW (0.10 nM) after incubation with varying amount of Atto-594 labeled anti-SUMO Affimer (dye label per Affimer = 0.35). (D) A plot of the FRET efficiency (E) v.s. dye/QR molar ratio fitted by a single QR donor in FRET interaction with N acceptors model, $E = I/[I+(r/R_0)^6/N]$.¹¹ Using a Förster radii (R_0) of 5.5 nm for QR-Atto-594 FRET pair calculated below, the average QD-dye distance r was calculated as 5.9 ± 0.2 nm.

It should be noted that our QR system is rod shaped, not spherical. Thus Affimers (with Atto-594 label) assembled on different sites on the QR would have quite different r values respective to the CdSe core at the centre of the QR (see EDX element mapping, ESI, **Fig. S1**). Given the inverse 6th power dependence of the E on r , the observed E would thus represent mainly Affimers assembled at the rod centre next to the CdSe core. Those assembled at the rod ends would contribute very little to the observed FRET and hence would be largely ignored.

The spectral overlap function between the QR emission and Atto-594 absorption is given by:¹²

$$J_{(\lambda)} = \frac{\int \text{PL}_{D(\lambda)} \varepsilon_{A(\lambda)} \lambda^4 d\lambda}{\int \text{PL}_{D(\lambda)} d\lambda}$$

Where $\text{PL}_{D(\lambda)}$ is the normalised QR fluorescence at λ ; $\varepsilon_{A(\lambda)}$ is the absorption coefficient of Atto-594 at λ . The integral of the spectral overlap for QD-Atto-594: $I = 3.18 \times 10^{15}$ (nm⁴.cm⁻¹.M⁻¹)

The original quantum yield (QY) of this batch of CdSe/CdS QR was 68% (provided by the supplier), and the UV light activated QR-ZW retained ~82% of its original QY (ESI, **Fig. S5E**), giving a QY of ~56% for the QR-ZW. Assuming a refractive index of 1.40 for the medium and random orientation of the dipoles ($K^2 = 2/3$), the Förster radius (R_0 , in the unit of Å) of the QR-Atto-594 FRET pair (at 1:1 molar ratio) can be calculated as follows:^{12,13}

$$R_0 = (8.79 \times 10^{-5} n_r^{-4} \times \text{QY} \times K^2 \times I)^{1/6}$$

$$R_0 = (8.79 \times 10^{-5} \times 1.40^{-4} \times 0.56 \times (2/3) \times 3.18 \times 10^{15})^{1/6}$$

$$= 54.8 \text{ \AA}$$

$$= 5.48 \text{ nm}$$

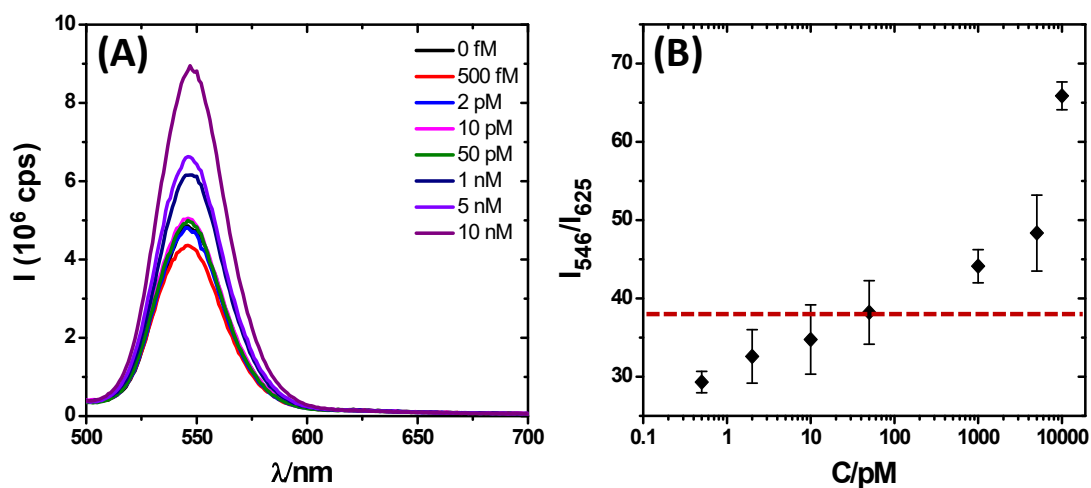


Figure S8. (A) Fluorescence spectra ($\lambda_{\text{EX}} = 450$ nm) of the QR-Affimer conjugate (0.10 nM) containing 0.10 nM Atto-594 labelled SUMO protein as FRET reporter after adding increasing amounts of unlabeled SUMO protein. (B) A plot of I_{546}/I_{625} ratio *versus* the unlabeled SUMO concentration (the broken red line shows the detection limit, background + 3σ).

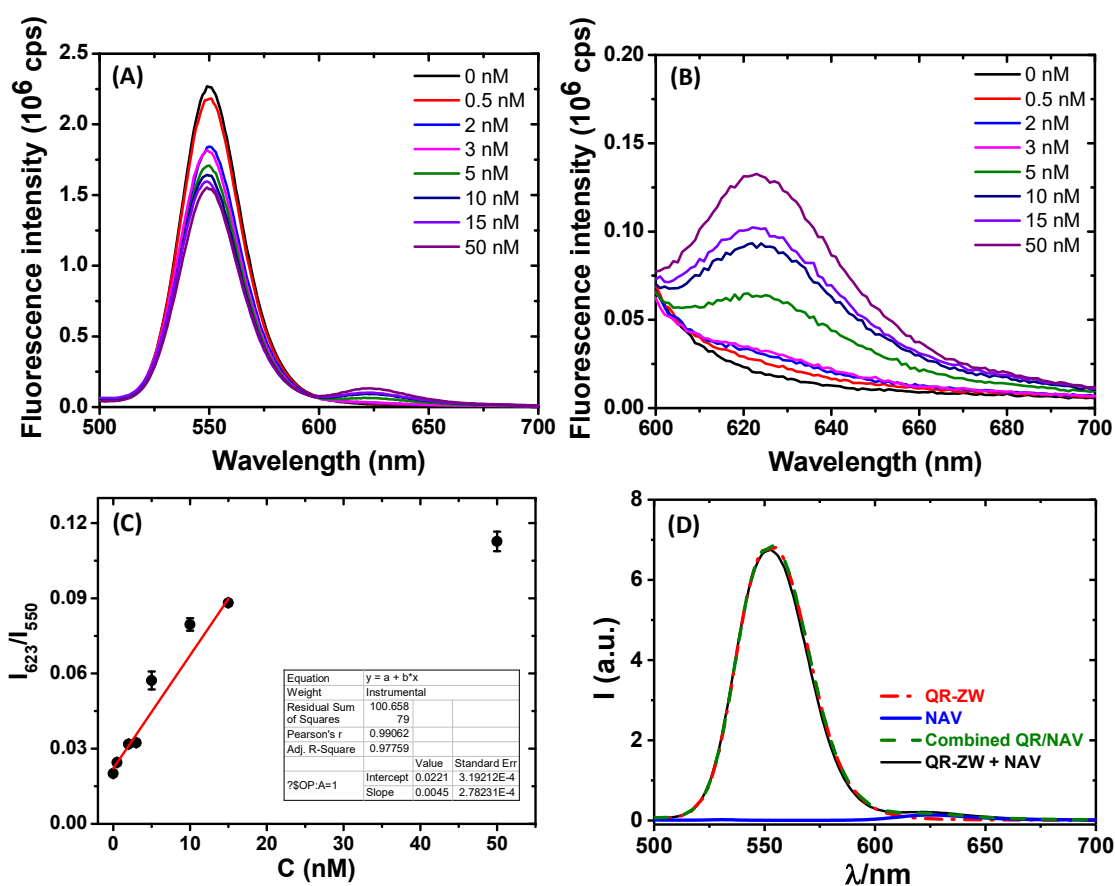


Figure S9. (A) Fluorescence spectra ($\lambda_{EX} = 450$ nm) of the QR-biotin₁₀₀ (0.5 nM QR) after incubation with different amount of Atto-594 labeled neutravidin in PBS containing a large excess of a non-target protein (bovine serum albumin, ~ 1.5 μ M). (B) Amplified fluorescence spectra in Atto-594 FRET region of 600 to 700 nm. (C) A plot of the I_{625}/I_{550} ratio *versus* neutravidin concentration, data from 0-15 nM were fitted by a linear function, $y = 0.0221 + 0.0045 x$, $R^2 = 0.978$. (D) Fluorescence spectra ($\lambda_{EX} = 450$ nm) of a DHLA-ZW ligand capped control QR (QR-ZW, 1 nM, broken red line), labeled neutravidin only (100 nM, solid blue line) and their physical mixture (solid black line). The simple sum of QR-ZW and labeled neutravidin spectra (broken green line) matches very well to that recorded from the QR-ZW + labeled neutravidin mixture, suggesting no nonspecific interaction between them (otherwise significant FRET signal would have been produced).

References

- (1) Guo, Y.; Sakonsinsiri, C.; Nehlmeier, I.; Fascione, M. A.; Zhang, H.; Wang, W.; Poehlmann, S.; Turnbull, W. B.; Zhou, D. *Angew. Chem. Int. Ed.* **2016**, *55*, 4738.
- (2) Song, L.; Ho, V. H. B.; Chen, C.; Yang, Z.; Liu, D.; Chen, R.; Zhou, D. *Adv. Healthcare Mater.* **2013**, *2*, 275; Kong, Y.; Chen, J.; Fang, H. W.; Heath, G.; Wo, Y.; Wang, W.; Li, Y. X.; Guo, Y.; Evans, S. D.; Chen, S.; Zhou, D. *Chem. Mater.* **2016**, *28*, 3041.
- (3) Susumu, K.; Mei, B. C.; Mattoussi, H. *Nat. Protoc.* **2009**, *4*, 424.
- (4) Zhan, N.; Mattoussi, H. *ACS Appl. Mater. Interfaces* **2013**, *5*, 2861.
- (5) Wang, W.; Guo, Y.; Tiede, C.; Chen, S.; Kopytynski, M.; Kong, Y.; Kulak, A.; TomLinson, D.; Chen, R.; McPherson, M.; Zhou, D. *ACS Appl. Mater. Interfaces* **2017**, *9*, 15232.
- (6) Tiede, C.; Tang, A. A. S.; Deacon, S. E.; Mandal, U.; Nettleship, J. E.; Owen, R. L.; George, S. E.; Harrison, D. J.; Owens, R. J.; TomLinson, D. C.; McPherson, M. J. *Protein Engin. Des. Select.* **2014**, *27*, 145.
- (7) Product information of netravadin: <https://www.thermofisher.com/order/catalog/product/31000>.
- (8) Zhang, Y.; Yuan, S. W.; Lu, R.; Yu, A. C. *J. Phys. Chem. B*, 2013, **117**, 7308-7316.
- (9) Y. Guo, I. Nehlmeier, E. Poole, C. Sakonsinsiri, N. Hondow, A. Brown, Q. Li, S. Li, J. Whitworth, Z. Li, A. Yu, R. Brydson, W. B. Turnbull, S. Pohlmann and D. Zhou, *J. Am. Chem. Soc.*, 2017, *139*, 11833-11844.
- (10) See lattice constants of solid materials:
https://7id.xray.aps.anl.gov/calculators/crystal_lattice_parameters.html
- (11) Medintz, I. L.; Mattoussi, H. *Phys. Chem. Chem. Phys.*, **2009**, *11*, 17.
- (12) Charbonniere, L. J.; Hildebrandt, N. *Eur. J. Inorg. Chem.* **2008**, *2008*, 3241.
- (13) Petryayeva, E.; Algar, W. R.; Medintz, I. L. *Appl. Spectros.*, **2013**, *67*, 215.